e-ISSN: 2550-164X

Available online at
https://jmeche.uitm.edu.my/

Journal of Mechanical Engineering 23(1) 2026, 116 – 131.

Journal of Mechanical Engineering

Microstructural Refinement and Texture Enhancement of ER 5356 Aluminium Alloy by Hybrid WAAM-Forging

Nornisaadila Musa[1,2], Mohd Shahriman Adenan[1*,2], Juri Sadeon[2]

[1]*Smart Manufacturing Research Institute, Universiti Teknologi MARA, 40450 Shah Alam, Selangor, Malaysia*
[2]*Faculty of Mechanical Engineering, Universiti Teknologi MARA, 40450 Shah Alam, Selangor, Malaysia*

ARTICLE INFO

Article history:
Received 17 June 2025
Revised 07 October 2025
Accepted 15 October 2025
Online first
Published 15 January 2026

Keywords:
Wire arc additive manufacturing
ER 5356 aluminium alloy
Hybrid manufacturing
Cold forging
Crystallography

DOI:
10.24191/jmeche.v23i1.7015

ABSTRACT

Wire arc additive manufacturing (WAAM) is a promising technique for fabricating aluminium alloy components due to their high strength-to-weight ratio and good machinability. However, challenges such as porosity and the formation of coarse columnar grains occurring from rapid solidification hinder its broader application. This study investigates a hybrid WAAM-forging approach with the aim of reducing porosity and modifying crystallographic texture in ER5356 aluminium alloy. Comparative analyses were conducted on as-deposited and WAAM-forged samples using scanning electron microscopy (SEM), electron backscatter diffraction (EBSD), and density analysis for characterisation. Results indicate that WAAM-forging significantly refines grain structure, mitigates columnar grain alignment, and promotes more homogeneous texture distribution. Kernel average misorientation (KAM) analysis reveals a lower degree of local misorientation in forged samples, suggesting effective stress relaxation. The pole figure analysis confirms a suppression of strong texture components, particularly in the {100} and {111} orientations, potentially reducing anisotropy in mechanical properties. The hybrid WAAM-forging process demonstrates significant improvements in the structural integrity and performance of WAAM-fabricated aluminium components, particularly through a reduction of porosity from 4.05% to 2.13% and a refinement of grain size from 168 µm to 122 µm. These findings contribute to the advancement of hybrid additive manufacturing strategies for high-performance applications.

INTRODUCTION

Wire arc additive manufacturing (WAAM) has been recognised by ASTM F2792-12a as a type of direct energy deposition (DED) that uses an electric arc as the heat source and a metal wire as the feedstock material (Rodrigues et al., 2019). WAAM has gained increasing interest across industrial sectors and

[1*] Corresponding author. *E-mail address*: mshahriman@uitm.edu.my
https://doi.org/10.24191/jmeche.v23i1.7015

research institutions due to its cost-effectiveness and suitability for fabricating large and complex metal components. Recent applications include critical sectors such as aerospace, marine, and transportation, with a growing focus on aluminium, steel alloys, and titanium (Vimal et al., 2021).

Aluminium alloys are particularly attractive due to their high strength-to-weight ratio, corrosion resistance, and recyclability, making them ideal for structures requiring long service life and reduced maintenance (Tonelli et al., 2021; Vimal et al., 2021). WAAM offers a significant advantage in producing large aluminium components at lower costs compared to conventional subtractive manufacturing techniques. However, the process is facing challenges, especially with the porosity that becomes a critical issue, primarily due to the hydrogen entrapment during solidification (Vimal et al., 2021). This phenomenon occurs in aluminium alloys when hydrogen solubility in the liquid phase is significantly higher than in the solid, leading to pore formation during rapid solidification (Langelandsvik et al., 2021).

Recent studies have shown significant focus on 5000 series aluminium alloys, such as ER5356, due to their high corrosion resistance, especially in marine environments. These alloys are magnesium-rich with added manganese to enhance corrosion resistance (Vijayakumar et al., 2021; Wieczorowski et al., 2023). Despite the advantages, WAAM-fabricated 5000 series components often suffer from microstructural inhomogeneity, extensive porosity, and coarse columnar grain structures, resulting from the complex thermal cycles intrinsic to the layer-by-layer deposition process (Derekar et al., 2020; Geng et al., 2021; Tonelli et al., 2021). Studies have shown that processes like pulsed-MIG, while effective in deposition, introduce higher porosity due to increased hydrogen absorption from the elevated arc energy and prolonged cooling times (Derekar et al., 2020).

To overcome these challenges, hybrid manufacturing approaches that combine additive manufacturing with subtractive or deformation processes have appeared to be a promising solution. The potential of hybrid manufacturing has been proven in that it could integrate additive manufacturing (AM) with techniques such as rolling, forging, or machining to overcome limitations of singular standalone processes (Strong et al., 2018; Pragana et al., 2021). The integration of forging with Wire Arc Additive Manufacturing (WAAM) within a hybrid manufacturing framework has been shown to enable the production of components with high geometric flexibility and improved mechanical properties, while simultaneously minimizing material waste and reducing tooling costs (Hirtler et al., 2020).

Recent works have indicated the potential of such approaches to refine grain structures, relieve residual stress, reduce porosity, and achieve more isotropic mechanical properties (Pragana et al., 2021). For instance, studies by Bambach et al. (2020) and Zhang et al. (2022) demonstrated the benefits of combining AM with metal forming, while Zhang et al. (2023) indicated the ability to enhance surface finish and tensile behaviour from hybrid WAAM-milling subtractive methods. However, a detailed understanding of how post-deposition plastic deformation in forging affects the microstructure and crystallographic texture of WAAM-fabricated ER5356 aluminium alloy is still lacking. Despite recent advancements in hybrid WAAM-forming technologies, including WAAM-rolling for Inconel 718 (Zhang et al., 2022) and WAAM-milling for Mg/Al alloys (Zhang et al., 2023), systematic exploration of WAAM-forging for aluminium alloys, particularly ER5356, remains limited.

While previous studies have demonstrated that post-deposition plastic deformation can improve formability and density (Silva et al., 2017; Tao et al., 2023), these works primarily emphasize global mechanical properties rather than providing detailed microstructural insights. Moreover, less research employed electron backscatter diffraction (EBSD) to directly quantify texture evolution and local misorientation using Kernel Average Misorientation (KAM) maps on a hybrid manufacturing framework. This study advances the current knowledge by integrating EBSD, SEM, and Archimedes-based porosity analysis to link microstructural transformations with process parameters and offers new insights into how cold forging modifies crystallographic features such as grain refinement and texture intensity in WAAM-built ER5356 aluminium alloy, which are underrepresented in current hybrid AM literature.

https://doi.org/10.24191/jmeche.v23i1.7015

This study aims to fill this understanding gap by investigating a hybrid WAAM-forging process for ER5356 aluminium alloy. The primary objective is to examine the effect of post-process cold forging on the microstructural evolution, porosity characteristics, and crystallographic texture of WAAM-fabricated components. By integrating WAAM and cold forging, this work explores a viable hybrid route to enhance the mechanical performance and structural integrity of aluminium alloy parts intended for high-performance applications.

The novelty of this research lies in demonstrating how cold forging transforms the microstructure and crystallographic characteristics of WAAM-fabricated ER5356 aluminium. It reveals that forging induces grain fragmentation and dislocation accumulation, converting coarse columnar grains into refined, equiaxed structures with markedly reduced porosity. The study also shows refined crystallographic texture and reduced local misorientation, which promotes more isotropic mechanical behaviour and improved structural reliability.

MATERIALS AND METHODOLOGY

Materials and experimental setup

This study used ER5356 aluminium alloy, which was deposited onto Al6061 substrates using the Gas Metal Arc Welding (GMAW) process. ER5356 was chosen for its good strength, ductility, and corrosion resistance, making it suitable for structural applications in WAAM (Horgar et al., 2018). The filler wire has a diameter of 1.2 mm, and the substrate for deposition, Al6061, has dimensions of 130 x 60 x 25 mm. The substrate was rigidly clamped to reduce thermal distortion during deposition. The chemical compositions of both the filler wire and substrate were analysed using energy-dispersive X-ray spectroscopy (EDX) with the TEAM Software Suite, as shown in Table 1. Deposition was performed using an EWM Titan XQ R 500 Pulse D system paired with a FANUC Robot Arc Mate 100iD robotic arm for precision. Argon shielding gas (99.99% purity) was supplied at 15 L/min to maintain arc stability and prevent oxidation.

Each wall consisted of 90 layers, and the deposition parameters were adapted from a previous study that reported minimal porosity at travel speeds of 350 mm/min – 450 mm/min (Zhou et al., 2020). The selection of WAAM process parameters, specifically current (152 A), voltage (19.2 V), and travel speed (420 mm/min), was initially based on the study by Zhou et al. (2020), which reported reduced porosity and stable arc performance for aluminium alloys under similar conditions. However, to enhance the robustness of the parameter justification, these values should ideally be supported by a broader process window study or corroborated with additional recent literature (Wieczorowski et al., 2023; Derekar et al., 2020; Geng et al., 2021). The process efficiency has been reported to range between 0.8 and 0.9; therefore, a value of 0.8 was assumed for the WAAM process in this study (Wieczorowski et al., 2023). A multi-source rationale would reinforce the relevance of the selected parameters for achieving optimal deposition quality, dimensional consistency, and reduced defect formation in ER5356 aluminium WAAM builds. Details of the process parameters are listed in Table 2.

Fig 1 shows the experimental setup used for the WAAM process. A thin wall structure, reaching a maximum height of 110 mm, was fabricated using an alternating directional deposition strategy with a hatching approach. This strategy, illustrated in Fig 2(a), involved a single weld bead per layer to reduce thermal gradients and promote uniform layer build-up. The alternating pattern was employed to minimise residual stress accumulation during deposition. A schematic of the single-bead deposition strategy is shown in Fig 2(b), while the completed thin wall is detailed in Fig 2(c). This approach was designed to ensure dimensional accuracy and repeatability while controlling heat input, which plays a critical role in determining microstructure features such as porosity and mechanical properties like tensile strength. The

https://doi.org/10.24191/jmeche.v23i1.7015

interlayer dwell time was maintained at approximately 5 seconds between each deposited layer to ensure uniform thermal cycles and minimize the accumulation of residual stress.

Table 1. Chemical composition of ER5356 and Al6061 alloys (wt%)

Alloy	Al	Si	Fe	Cu	Mn	Mg	Zn	Cr	Ti
ER5356	91.4	0.3	0.4	1.1	0.3	5.6	-	0.6	0.3
Al6061	93.4	0.1	0.2	0.3	0.1	5.0	0.2	0.7	-

Table 2. WAAM parameters for GMAW process

Technique	Electrical parameter			Efficiency	Heat input
	Travel speed	Current range	Voltage		
GMAW	420 mm/min	152 A	19.2 V	0.8	307.47 J/mm

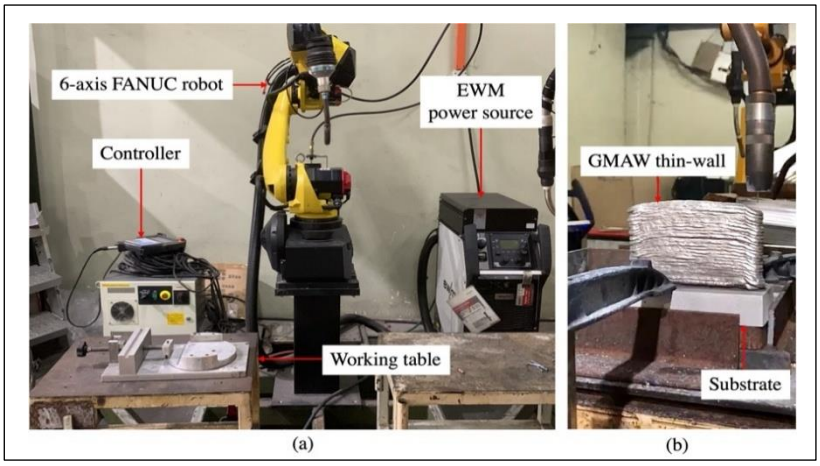

Fig. 1. GMAW setup for WAAM process (a) equipment arrangement and (b) formation of thin-wall structure.

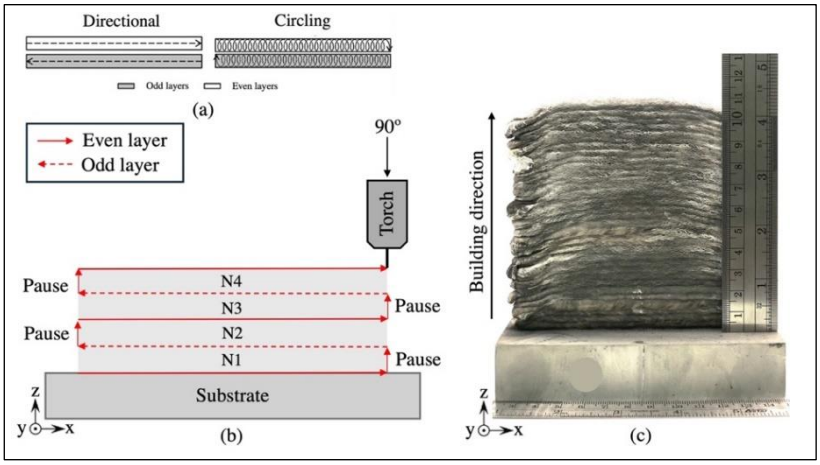

Fig. 2. WAAM deposition strategy: (a) deposition pattern types (Arana et al., 2021), (b) single weld bead per layer with hatching style and (c) fabricated thin-wall structure (128 x 20 x 110 mm).

https://doi.org/10.24191/jmeche.v23i1.7015

Cold forging process

After WAAM fabrication, the thin-wall structures were subjected to cold forging as a post-processing step to enhance mechanical properties, particularly porosity. The forging was performed on a J23-100 press machine (1000 kN capacity) using an open-die configuration at room temperature. Table 3 presents the cold forging parameters. Upsetting was carried out with different degrees of deformation, which are reductions in length of 2 mm and 4 mm. The maximum reduction length during the cold forging process was limited to 4 mm, as the preliminary experiments revealed that reductions exceeding this threshold induced significant bending and initiated cracking in the fabricated thin wall for the desired dimension (128 x 20 x 110 mm), thereby compromising the structural integrity of the samples. The selection of 2 mm and 4 mm deformation levels was based on preliminary forging trials to determine the threshold at which structural distortion or cracking begins to occur in WAAM-fabricated thin walls. Reductions beyond 4 mm induced significant bending and cracking due to geometric constraints and strain localization in the deposited layers. These values were therefore chosen to represent the upper limit of stable deformation without compromising sample integrity. From a practical standpoint, the selected reductions also reflect forging strains that are relevant in industrial post-processing for densification and grain refinement without extensive die redesign or re-fixturing. The process parameters were precisely controlled, including a forging speed of 25 mm/min and a stroke limit of 1 mm. A maximum load of 1000 kN was applied, generating a contact pressure of 390.65 MPa, which was three times higher than the yield strength of ER5356 (120 MPa), which was sufficiently able to plastically deform the aluminium alloy. This level of pressure facilitates effective pore closure and grain subdivision within the WAAM-deposited layers. The setup, including specimen placement on an SKH55 (AISI M35) spacer with a hardness of 65 HRC, is shown in Fig 3.

Table 3. Cold forging parameters

Machine	Temperature	Process type	Degree of deformation	Forging speed
J23-100 press machine (1000 kN)	Ambient	Upsetting	2 mm, 4mm	25 mm/min

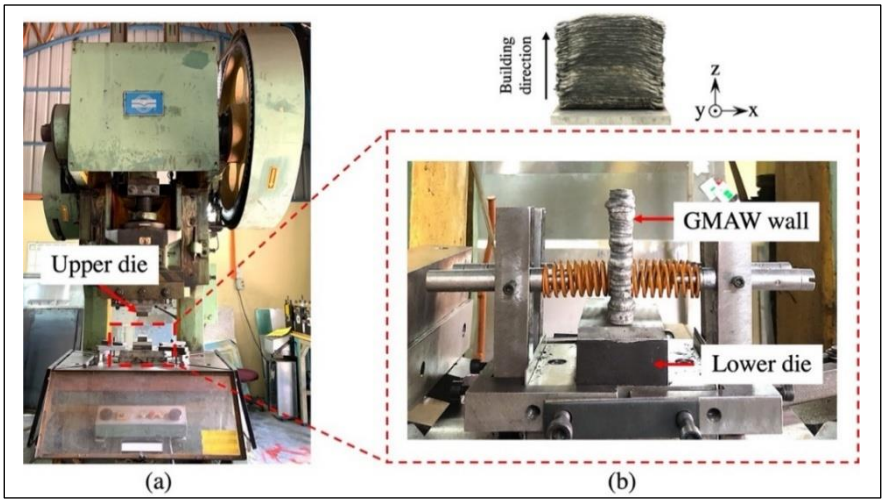

Fig. 3. Forging process setup for WAAM samples: (a) power press machine and (b) specimen placement for deformation.

https://doi.org/10.24191/jmeche.v23i1.7015

Density and porosity analysis

The density and porosity test of the specimens were assessed using Archimedes' principle in accordance with ISO 3369:2006 (Nawaz & Rani, 2021). This method provides an accurate and cost-effective way to quantify porosity (Yang et al., 2018), particularly for high-density metallic specimens fabricated by additive manufacturing (Bruce et al., 2022). Fig 4(a) shows the setup for the density test, which involved an analytical balance with 0.1 mg resolution, a beaker and a dual-weighing density pan to measure the specimen's mass in air and water.

Microstructure analysis and grain characterization

Microstructural characterisation was conducted to evaluate the deformation features, defect formation, and grain structure evolution in both as-built WAAM and hybrid WAAM-forged ER5356 aluminium samples. Three specimens were extracted from the mid-height region of the wall to ensure repeatability and representativeness measurement. Specimens were sectioned to 10 × 10 × 5 mm, refer to Fig 4(b), using an abrasive waterjet cutting process (Flow Mach 100) from the most stable deposition region to ensure consistency. Standard metallographic preparation was performed according to ASTM E3, involving sequential grinding with silicon carbide (SiC) papers and polishing with diamond suspensions down to 1 µm to produce a mirror-like surface finish.

Initial observations were carried out using a Hitachi SU3500 scanning electron microscope (SEM), enabling identification of voids, crack paths, and other deformation features, along with Hitachi EDX Quantax 70 Energy-X-ray Spectroscopy (EDX) for material elemental analysis. Additional microstructural inspection focusing on grain shape, porosity, and boundaries was performed using a JEOL JSM-6380LV SEM. Samples were ultrasonically cleaned in ethanol, then chemically etched in Keller's reagent, while for EBSD analysis, electropolishing in a perchloric acid-ethanol solution (1:10) at 25V for 20 seconds was used to enhance Kikuchi pattern clarity.

The EBSD measurements were conducted on an Oxford Instruments EBSD system integrated with AZtecHKL Advanced software. A step size of 1.2 µm was selected to effectively capture grain orientation and deformation characteristics, especially in the coarser grains typically found in WAAM-fabricated aluminium alloys. The average grain size in the observed region was calculated by the transverse scribing method in ImageJ software.

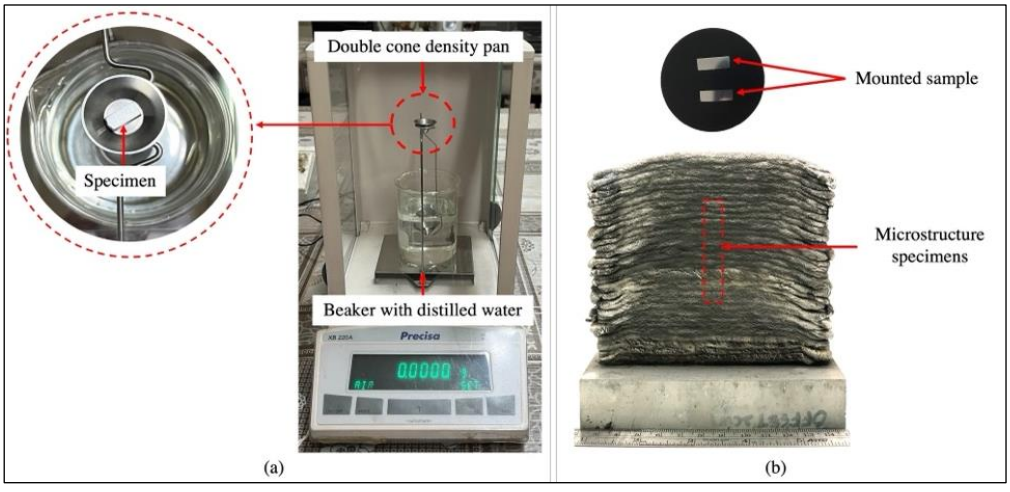

Fig. 4. (a) Setup for density measurement using Archimedes' method and (b) microstructure observation area and mounted specimens for SEM and EBSD analysis.

https://doi.org/10.24191/jmeche.v23i1.7015

RESULTS AND DISCUSSION

Porosity and elemental distribution via SEM/EDX

The initial assessment of porosity was conducted using SEM on the vertical cross-sections of WAAM and WAAM-forged samples. Fig 5 presents representative micrographs revealing that the WAAM samples exhibit a high concentration of spherical and irregular cavities and pores, and EDX was employed to analyse the chemical composition around the pores. The EDX analysis shows that the ER5356 consists of the key alloy elements of Al and Mg. The observed surface exhibits a lower content of Al compared to the filler wire composition. However, the values fall within the range of ER5356. Based on the micrograph in Fig 5(b), the porosity existed due to gas pores escaping from the melt pool, which caused cavities to be found in the walls as shown in Fig 5(a), leaving an open pore on the surface. The pores formed a spherical and homogeneous distribution with a diameter up to 100 μm into the big and inhomogeneously distributed pores. There are few factors that increase the formation of porosity during the WAAM process. Surface contaminants on wires and substrates, including moisture, dirt, grease, and hydrocarbons, are difficult to completely remove (Zhang et al., 2024). Thus, the melt pool easily devours these contaminants, absorbing energy during the deposition process and contributing to pore formation during solidification. Further reasons for the incorporation of air could be that the pores were in contact with oxygen, as shown in Fig 5(b) EDX analysis, where most likely the oxygen came from the ambient air and entered the process zone. It is also because of the recirculation effects (Hauser et al., 2021). Hence, these pores are commonly aligned along interlayer boundaries, which are regions of thermal instability and weak metallurgical bonding. In contrast, the WAAM-forged samples show a more compact surface morphology with reduced voids. The forging process applies compressive deformation normal to the build direction, which aids in collapsing internal voids and promoting interlayer fusion (Silva et al., 2017).

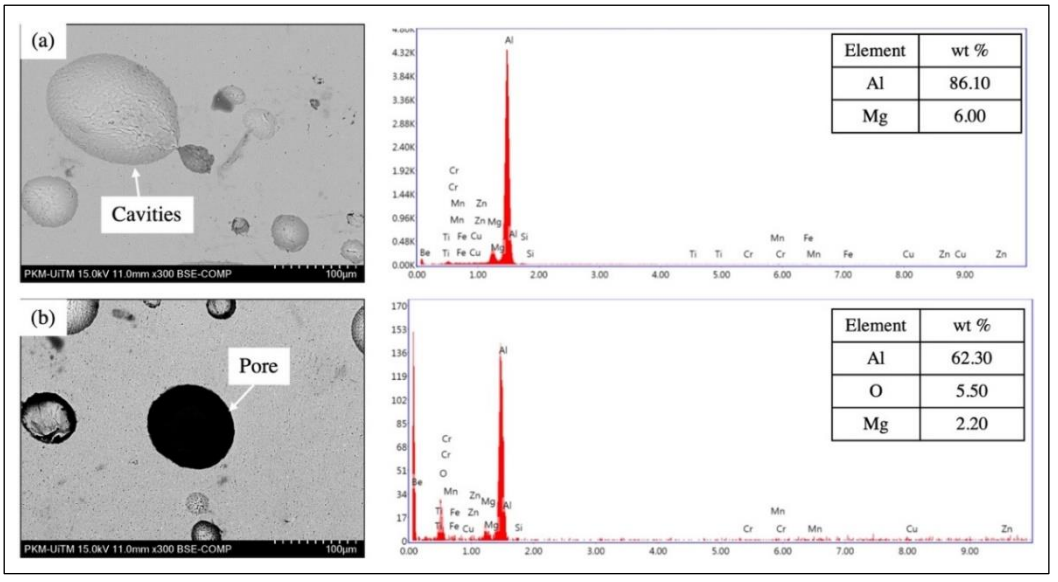

Fig. 5. SEM images of WAAM ER5356 showing (a) surface cavities from gas entrapment and (b) irregular pore distribution, indicating poor fusion between layers.

The EDX was used to analyse the chemical composition around the pores. The EDX maps after the WAAM (Fig 6) and WAAM-forged (Fig 7) processes also match the chemical composition with the filler wire. The WAAM and hybrid manufacturing of WAAM-forged maintained the composition of material

https://doi.org/10.24191/jmeche.v23i1.7015

after the processes, as in Figs 6(b) – 6(f) and Figs 7(b) – 7(f), respectively. However, because of the higher formation of pores, high oxygen content was detected around the porosity regions in WAAM samples in Fig 6(e), suggesting that oxidation and gas entrapment played significant roles in defect formation (Hauser et al., 2021; Zhang et al., 2024). While the EDX mapping in the WAAM-forged samples displayed a more uniform distribution of aluminium and magnesium, with significantly reduced oxygen, indicating effective minimal contamination from surrounding gas through the forging process.

To reduce the porosity percentage or content (PC), some studies suggest applying a hybrid manufacturing approach of WAAM and the forging process to achieve superior mechanical properties through plastic deformation and strain hardening by vertical compression force (Silva et al., 2017). Fig 8 shows the SEM observation of WAAM, WAAM-forged with 2 mm reduction (WF#2), and WAAM-forged with 4 mm reduction (WF#4). The SEM micrograph shows the existence of pores and cavities in almost all samples. Based on Fig 8(a), the PC of WAAM produces a higher value, which is 4.05%, compared to the WAAM-forged process in Figs 8(b) and 8(c). As the PC of WAAM-forged samples is lower than WAAM, the microstructure shows a better micrograph as the degree of deformation increases. The formation of cavities and porosity is reduced due to the upsetting press being parallel to the building direction (z-axis). The forging process led to the elimination of inter-particle boundaries and the squeezing of grains. Thus, the deformation-induced grain subdivision or refinement and dislocation accumulation occur in the material. To further quantify porosity, the density of each sample was determined using the Archimedes method in accordance with ISO 3369:2006. As detailed in Fig 4, WAAM samples recorded a density of 2.533 g/cm³, while WF#2 and WF#4 reached 2.586 g/cm³ and 2.585 g/cm³, respectively. In Fig 8(d), the density shows a non-uniform trend as the degree of deformation increases compared to the PC due to measurement limitations. There is a general assumption made that the method captures all internal volume inconsistencies, including microcracks and unfilled spaces (Jorge et al., 2023). However, the improved density in forged samples can be attributed to effective plastic deformation, which reduces porosity by consolidating deposited layers and increasing local compaction (Silva et al., 2017).

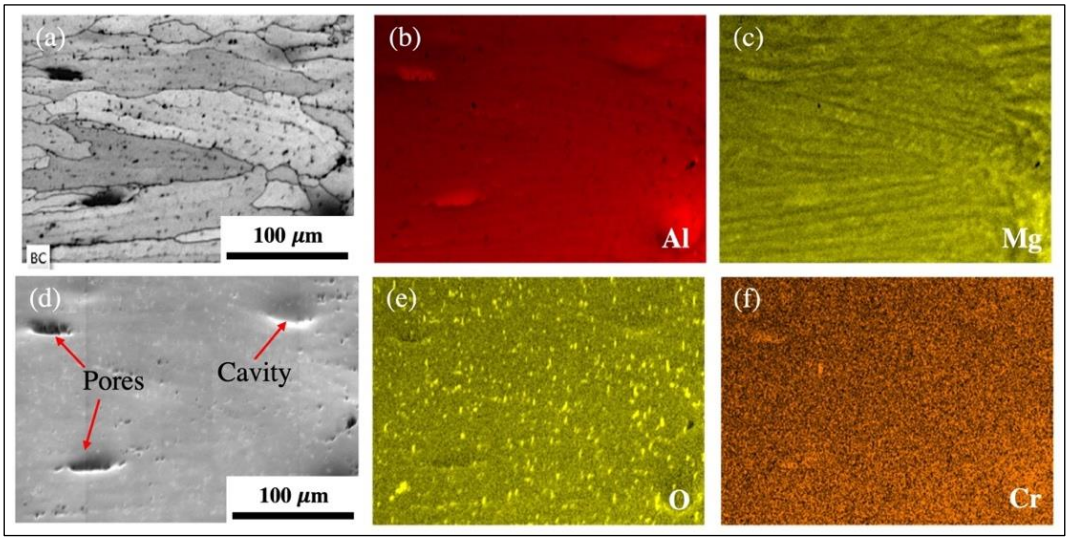

Fig. 6. EDX band contrast and elemental maps of WAAM sample (a) band contrast (BC) and (b) – (f) EDX maps showing elemental distribution and oxygen presence around pores.

https://doi.org/10.24191/jmeche.v23i1.7015

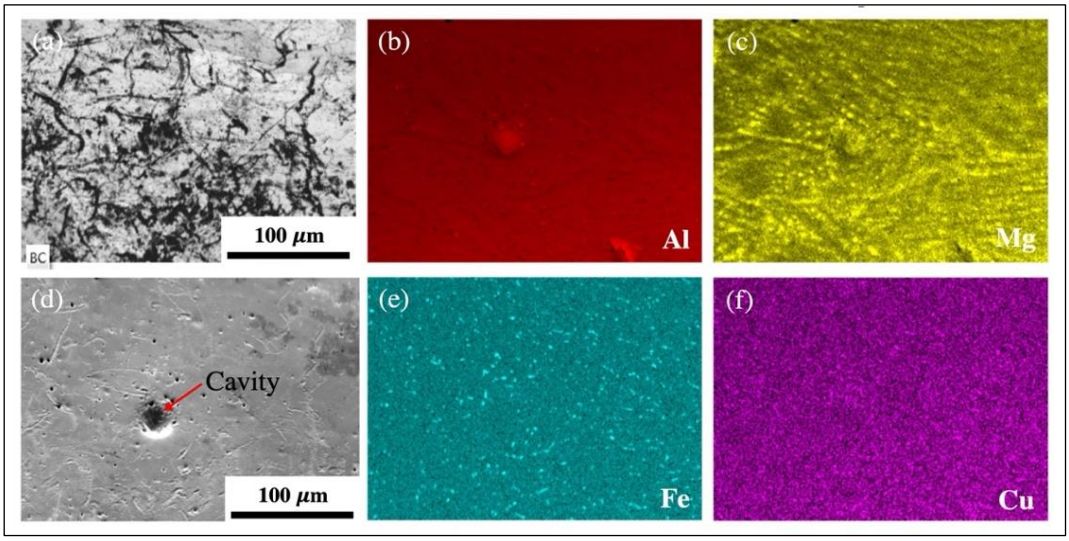

Fig. 7. EDX band contrast (BC) and elemental maps of WAAM-forged sample (a) band contrast (BC), and (b) – (f) EDX maps showing improved elemental uniformity after forging.

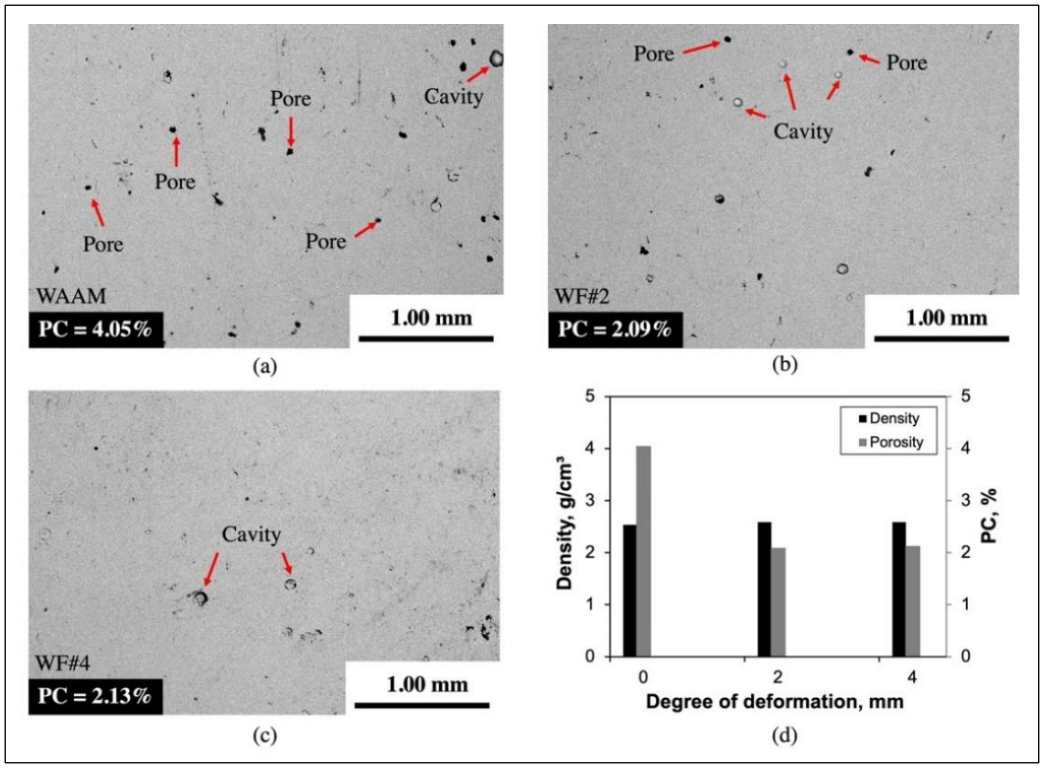

Fig. 8. SEM images comparing porosity in (a) WAAM, (b) WAAM-forged with 2 mm reduction, (c) WAAM-forged with 4 mm reduction, and (d) graph shows higher density and lower porosity with increased deformation.

https://doi.org/10.24191/jmeche.v23i1.7015

Forging imposes compressive forces that facilitate particle rearrangement and interlayer bonding. As shown in Fig 8, increasing the degree of deformation from 2 mm to 4 mm led to further porosity elimination and microstructural compactness. This effect is attributed to grain deformation and mechanical closure of voids during forging. Furthermore, reduced porosity corresponds with improved mechanical properties such as tensile strength and fatigue life, making forging a practical solution for enhancing WAAM components (Tao et al., 2023). To prove and validate the grain refinement of ER5356 after WAAM and WAAM-forging, the EBSD analysis is performed on WAAM and WF#4 for further details.

Grain refinement and morphological transformation through forging post-process

Grain morphology was analysed using EBSD in the vertical (cross-sections) direction to understand the microstructural transformations due to forging. The region is chosen from the middle of the deposited sample, as shown in Fig 9(a) for WAAM and WAAM-forged samples. Fig 9(b) illustrates that WAAM samples consist of coarse, elongated columnar grains that grow in the direction of deposition (x-axis). The average grain size in this region was calculated to be approximately 168 µm. This morphology results from directional solidification, where a steep thermal gradient exists along the deposition path. Repeated thermal cycles worsen grain coarsening, particularly in the middle layers that experience slower cooling rates due to thermal accumulation (Li et al., 2020a; Li et al., 2020b). In contrast, the WF#4 samples, as shown in Fig 9(c), exhibit equiaxed grain structures with significantly smaller sizes. The average grain size decreased to 122 µm, indicating grain refinement due to dislocation accumulation. This transition from columnar to equiaxed grains is a result of dislocation pile-up and grain subdivision, which are driven by the plastic strain introduced during forging. These refined structures improve isotropy and enhance mechanical properties, as grain boundaries act as barriers to crack propagation and dislocation movement (Li et al., 2023).

The microstructural transition not only reduces grain size but also contributes to isotropic mechanical behaviour. Columnar grains in WAAM samples lead to directional anisotropy where strength and ductility vary with orientation. Forging interrupts this grain alignment, producing more uniform, isotropic microstructures. This structural uniformity is essential in aerospace and marine applications where components are subjected to multi-directional loads (Li et al., 2020a).

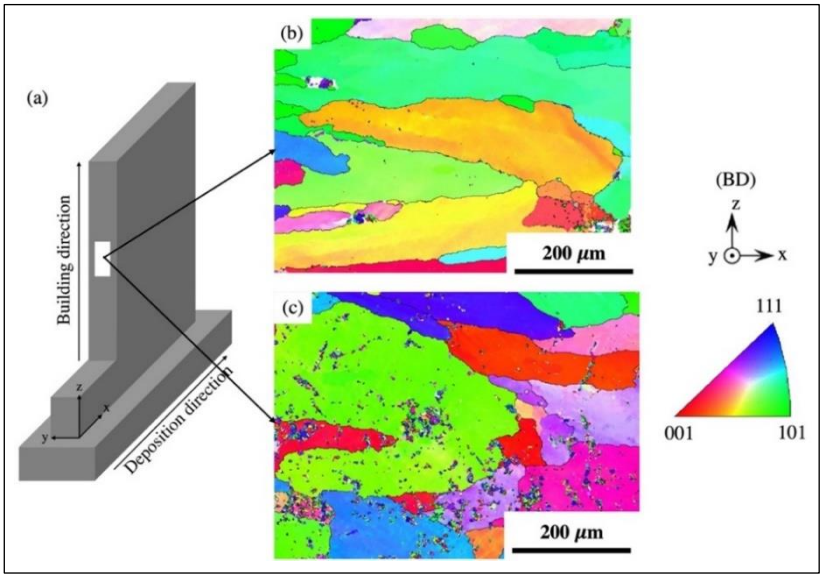

Fig. 9. EBSD maps showing (a) scan area, (b) columnar grains in WAAM and (c) finer equiaxed grains in forged sample confirming grain refinement due to forging.

https://doi.org/10.24191/jmeche.v23i1.7015

Plastic deformation behavior and dislocation density

Kernel Average Misorientation (KAM) maps were used to assess the degree of plastic deformation in both WAAM and WF#4 samples. Fig 10(a) reveals that WAAM samples had low KAM values, indicating low local misorientation and dislocation density. This aligns with the absence of mechanical working post-deposition. In contrast, WF#4 samples, as seen in Fig 10(b), displayed elevated KAM values, especially in regions subjected to a high degree of deformation. This increase is attributed to strain-induced dislocation generation and rearrangement within the microstructure (Bouquerel et al., 2015). The highest local misorientation for the WAAM sample was 2.395417, and for the WF#4 was 1.30336, indicating higher stored strain and dislocation density in the as-deposited WAAM. Higher KAM values suggest increased geometrically necessary dislocations (GNDs), which indicate plastic strain accumulation. These dislocations arise from forging-induced deformation, promoting sub-grain formation. The increase in internal strain energy enhances the potential for grain refinement, consistent with observations in Fig 9. The transformation of microstructure through the dislocation-driven processes is critical to improve ductility, toughness, and fatigue resistance (Khan & Mohan, 2020).

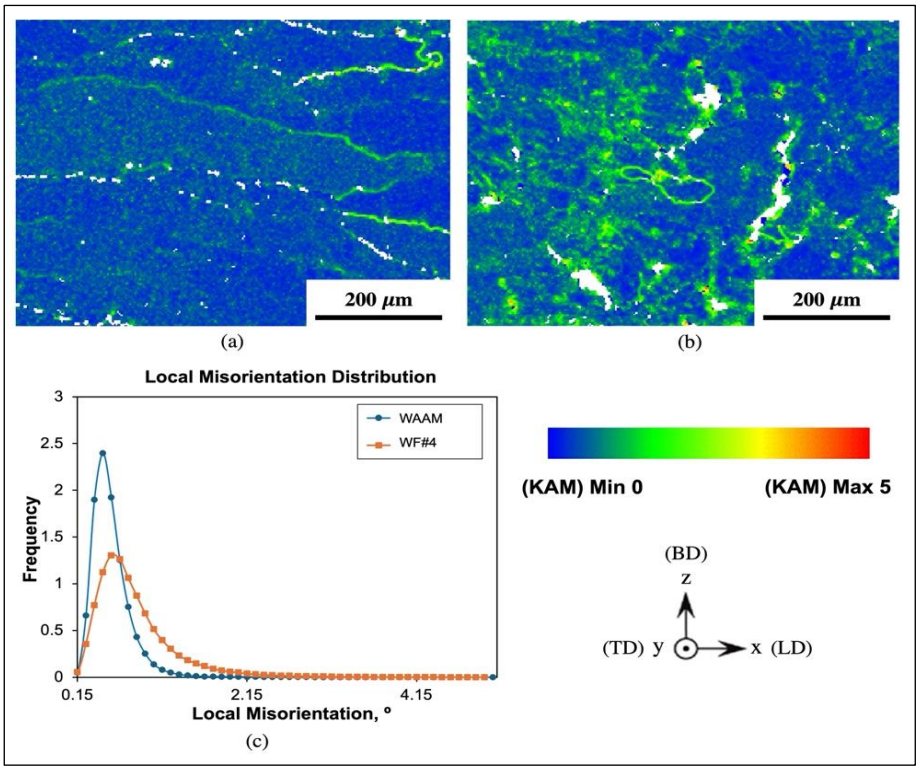

Fig. 10. KAM maps orientation of ER5356 (a) WAAM samples, (b) WAAM-forged sample, and (c) frequency distribution of local misorientation.

Texture strengthening and anisotropy reduction in WAAM-forged microstructure

Pole figure analysis was used to assess the crystallographic texture of the samples. WAAM samples indicated weak and scattered textures across the {100}, {110}, and {111} planes, as seen in Figs 11(a) – 11(c). This indicates a lack of preferred orientation due to rapid solidification and the random nucleation of grains. Weak textures often lead to inconsistent mechanical properties and poor anisotropy control (Li

https://doi.org/10.24191/jmeche.v23i1.7015

et al., 2020a). Meanwhile, WAAM-forged samples showed more obvious textures, particularly in the {100} and {111} directions, as shown in Figs 11(d) – 11(f). The maximum texture intensity increased from 14.11 in WAAM to 22.59 in WAAM-forged samples. This enhancement results from strain-induced grain rotation and selective growth. Preferable alignment of grains along specific crystallographic planes is a known outcome of plastic deformation in aluminium alloys (Li et al., 2023). The development of crystallographic texture plays a critical role in tailoring mechanical properties. Enhanced texture in WF#4 samples indicates better control over directional strength, ductility, and fatigue performance. Texture sharpening also reduces anisotropy, which is a significant limitation in as-built WAAM parts. By aligning grains along favourable orientations, forging improves load-bearing capacity and extends component life under cyclic loading conditions (Li et al., 2023).

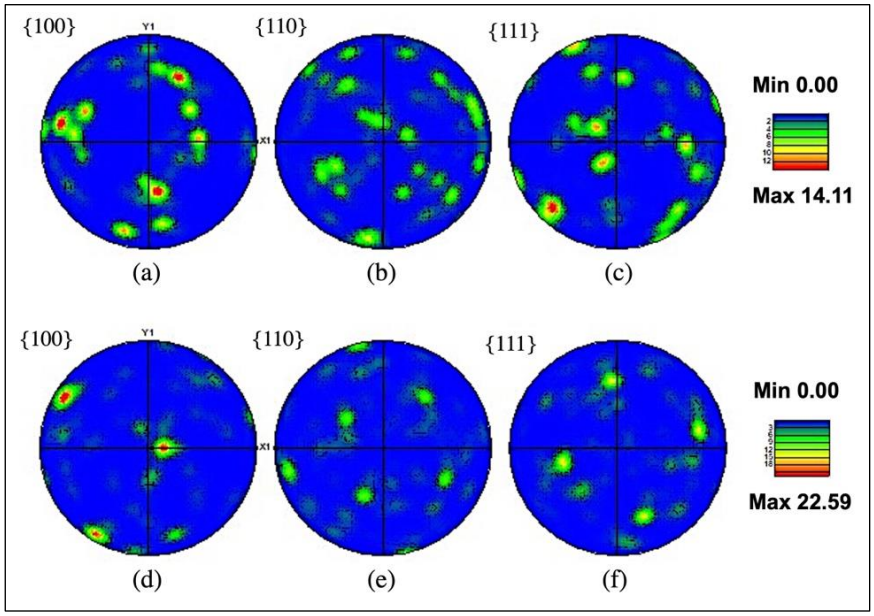

Fig. 11. Pole figures showing grain orientation in WAAM (a–c) and forged (d) – (f) samples. Forging sharpens texture, improving grain alignment and reducing anisotropy.

CONCLUSION

In the present work, the effects of hybrid WAAM-forged on the microstructural characteristics and crystallographic texture of ER5356 aluminium alloy are studied. The comparative analysis between WAAM and WAAM-forged samples revealed significant improvements in the microstructure due to the forging step. Based on the experimental results, the forging process effectively reduced porosity in WAAM components. SEM and density measurements confirmed that forging promoted better particle rearrangement and pore closure, resulting in increased material density, and improved microstructural integrity. EBSD analysis revealed a clear transformation from coarse, columnar grains in WAAM samples to refined, equiaxed grains in WAAM-forged specimens. This refinement contributed to a more homogeneous and isotropic microstructure. KAM maps showed a significant increase in local misorientation and dislocation density in forged samples, indicating effective strain accumulation and plastic deformation. These features are beneficial for improving toughness and resistance to fatigue failure. Crystallographic texture analysis demonstrated stronger grain orientation in the {100} and {111} planes

https://doi.org/10.24191/jmeche.v23i1.7015

after forging. This texture sharpening enhances directional mechanical properties and reduces anisotropy, supporting improved load-bearing behaviour under multi-axial stresses.

The hybrid WAAM-forging process significantly enhances the microstructural homogeneity, reduces porosity, refines grains, and improves the crystallographic texture of the ER5356 alloy. These findings highlight the effectiveness of post-deposition deformation in mitigating WAAM-induced defects, making hybrid WAAM-forging a promising approach for high-performance structural applications. While this study employed Archimedes' method and SEM imaging to evaluate porosity, these techniques provide limited insight into internal pore morphology and volumetric distribution. For more rigorous validation, future work should incorporate quantitative image analysis using thresholding on cross-sectional micrographs to estimate pore area fraction. Additionally, non-destructive 3D porosity mapping using X-ray computed tomography (micro-CT) is recommended to capture internal pore structure, spatial distribution, and connectivity. Such approaches would enable a more accurate correlation between process-induced defects and mechanical performance in WAAM-forged components. Although the combination of WAAM and forging may be used to develop a new hybrid manufacturing process, future work needs to validate the metallography characterisation. Reducing the heat input can improve the microstructure and reduce the porosity of the aluminium alloy. The heat input range can be tested in different combinations of travel speed and cooling time.

ACKNOWLEDGEMENTS/ FUNDING

The authors would like to acknowledge the Ministry of Higher Education (MOHE) for funding under the Geran Konsortium Kecemerlangan Penyelidikan (Hybrid Manufacturing: Integration of Direct Energy Deposition (DED) Wire-Arc Additive Manufacturing (WAAM) with Forging Operations for Production of Net Shaped Lightweight Metal Alloy Components), 600-RMC/KKP 5/3 (003/2021) and express gratitude to the staff member of Smart Manufacturing Research Institute (SMRI) as well as staff of the Welding Laboratory, Advanced Manufacturing Laboratory and Material Laboratory at Faculty of Mechanical Engineering, Universiti Teknologi MARA (UiTM) Shah Alam.

CONFLICT OF INTEREST

The authors agree that this research was conducted in the absence of any self-benefits, commercial or financial conflicts, and declare the absence of conflicting interests with the funders.

AUTHORS' CONTRIBUTION

The authors confirm equal contribution in each part of this work. All authors reviewed and approved the final version of this work.

REFERENCES

Arana, M., Ukar, E., Rodriguez, I., Iturrioz, A., & Alvarez, P. (2021). Strategies to reduce porosity in Al-Mg WAAM parts and their impact on mechanical properties. Metals, 11(3), 524. https://doi.org/10.3390/met11030524

https://doi.org/10.24191/jmeche.v23i1.7015

Bambach, M., Sizova, I., Sydow, B., Hemes, S., & Meiners, F. (2020). Hybrid manufacturing of components from Ti-6Al-4V by metal forming and wire-arc additive manufacturing. Journal of Materials Processing Technology, 282, 116689. https://doi.org/10.1016/j.jmatprotec.2020.116689

Bouquerel, J., Diawara, B., Dubois, A., Dubar, M., Vogt, J. B., & Najjar, D. (2015). Investigations of the microstructural response to a cold forging process of the 6082-T6 alloy. Materials and Design, 68, 245-258. https://doi.org/10.1016/j.matdes.2014.12.005

Bruce, D., Paradise, P., Saxena, A., Temes, S., Clark, R., Noe, C., Benedict, M., Broderick, T., & Bhate, D. (2022). A critical assessment of the Archimedes density method for thin-wall specimens in laser powder bed fusion: measurement capability, process sensitivity and property correlation. Journal of Manufacturing Processes, 79, 185–192. https://doi.org/10.1016/j.jmapro.2022.04.059

Derekar, K. S., Addison, A., Joshi, S. S., Zhang, X., Lawrence, J., Xu, L., Melton, G., & Griffiths, D. (2020). Effect of pulsed metal inert gas (Pulsed-MIG) and cold metal transfer (CMT) techniques on hydrogen dissolution in wire arc additive manufacturing (WAAM) of aluminium. International Journal of Advanced Manufacturing Technology, 107(1–2), 311–331. https://doi.org/10.1007/s00170-020-04946-2

Geng, Y., Panchenko, I., Chen, X., Ivanov, Y., & Konovalov, S. (2021). Investigation of microstructure and fracture mechanism of Al-5.0Mg alloys fabricated by wire arc additive manufacturing. Journal of Materials Engineering and Performance, 30(10), 7406–7416. https://doi.org/10.1007/s11665-021-05973-0

Hauser, T., Reisch, R. T., Breese, P. P., Lutz, B. S., Pantano, M., Nalam, Y., Bela, K., Kamps, T., Volpp, J., & Kaplan, A. F. H. (2021). Porosity in wire arc additive manufacturing of aluminium alloys. Additive Manufacturing, 41, 101993. https://doi.org/10.1016/j.addma.2021.101993

Hirtler, M., Jedynak, A., Sydow, B., Sviridov, A., & Bambach, M. (2020). A study on the mechanical properties of hybrid parts manufactured by forging and wire arc additive manufacturing. Procedia Manufacturing, 47, 1141–1148. https://doi.org/10.1016/j.promfg.2020.04.136

Horgar, A., Fostervoll, H., Nyhus, B., Ren, X., Eriksson, M., & Akselsen, O. M. (2018). Additive manufacturing using WAAM with AA5183 wire. Journal of Materials Processing Technology, 259, 68–74. https://doi.org/10.1016/j.jmatprotec.2018.04.014

Jorge, V. L., Teixeira, F. R., Scotti, A., Scotti, F. M., & Siewert, E. (2023). The significance of supplementary shielding in WAAM of aluminium thin walls. Journal of Manufacturing Processes, 106, 520–536. https://doi.org/10.1016/j.jmapro.2023.09.063

Khan, A., & Mohan, R. (2020). Change in the mechanical and electrical properties of aluminium 6063 alloy under cold forging process. International Research Journal of Engineering and Technology, 7(12), 476–478.

Langelandsvik, G., Akselsen, O. M., Furu, T., & Roven, H. J. (2021). Review of aluminum alloy development for wire arc additive manufacturing. Materials, 14(18), 5370. https://doi.org/10.3390/ma14185370

Li, H., Wang, L., He, W., Cheng, L., Chen, J., & Yi, L. (2023). Effect of cold pressing deformation on microstructure and residual stress of 7050 aluminum alloy die forgings. Materials, 16(14), 5129. https://doi.org/10.3390/ma16145129

Li, S., Zhang, L. J., Ning, J., Wang, X., Zhang, G. F., Zhang, J. X., & Na, S. J. (2020). Microstructures and mechanical properties of Al-Zn-Mg aluminium alloy samples produced by wire + arc additive manufacturing. Journal of Materials Research and Technology, 9(6), 13770–13780.

https://doi.org/10.24191/jmeche.v23i1.7015

https://doi.org/10.1016/j.jmrt.2020.09.114

Li, S., Zhang, L. J., Ning, J., Wang, X., Zhang, G. F., Zhang, J. X., Na, S. J., & Fatemeh, B. (2020). Comparative study on the microstructures and properties of wire + arc additively manufactured 5356 aluminium alloy with argon and nitrogen as the shielding gas. Additive Manufacturing, 34, 101206. https://doi.org/10.1016/j.addma.2020.101206

Nawaz, A., & Rani, S. (2021). Fabrication and evaluation of percent porosity and density reduction of aluminium alloy foam. Materials Today: Proceedings, 47(17), 6025–6029. https://doi.org/10.1016/j.matpr.2021.04.607

Pragana, J. P. M., Sampaio, R. F. V., Bragança, I. M. F., Silva, C. M. A., & Martins, P. A. F. (2021). Hybrid metal additive manufacturing: a state–of–the-art review. Advances in Industrial and Manufacturing Engineering, 2, 100032. https://doi.org/10.1016/j.aime.2021.100032

Rodrigues, T. A., Duarte, V., Miranda, R. M., Santos, T. G., & Oliveira, J. P. (2019). Current status and perspectives on wire and arc additive manufacturing (WAAM). Materials, 12(7), 1121. https://doi.org/10.3390/ma12071121

Silva, C. M. A., Bragança, I. M. F., Cabrita, A., Quintino, L., & Martins, P. A. F. (2017). Formability of a wire arc deposited aluminium alloy. Journal of the Brazilian Society of Mechanical Sciences and Engineering, 39(10), 4059–4068. https://doi.org/10.1007/s40430-017-0864-z

Strong, D., Kay, M., Conner, B., Wakefield, T., & Manogharan, G. (2018). Hybrid manufacturing – integrating traditional manufacturers with additive manufacturing (AM) supply chain. Additive Manufacturing, 21, 159–173. https://doi.org/10.1016/j.addma.2018.03.010

Tao, L., Feng, Z., Jiang, Y., & Tong, J. (2023). Analyzing forged quality of thin-walled A-286 superalloy tube under multi-stage cold forging processes. Materials, 16(13), 4598. https://doi.org/10.3390/ma16134598

Tonelli, L., Laghi, V., Palermo, M., Trombetti, T., & Ceschini, L. (2021). AA5083 (Al–Mg) plates produced by wire-and-arc additive manufacturing: effect of specimen orientation on microstructure and tensile properties. Progress in Additive Manufacturing, 6(3), 479–494. https://doi.org/10.1007/s40964-021-00189-z

Vijayakumar, M. D., Dhinakaran, V., Sathish, T., Muthu, G., & Ram, P. M. B. (2021). Experimental study of chemical composition of aluminium alloys. Materials Today: Proceedings, 37(2), 1790–1793. https://doi.org/10.1016/j.matpr.2020.07.391

Vimal, K. E. K., Srinivas, M. N., & Rajak, S. (2021). Wire arc additive manufacturing of aluminium alloys: a review. Materials Today: Proceedings, 41(5), 1139–1145. https://doi.org/10.1016/j.matpr.2020.09.153

Wieczorowski, M., Pereira, A., Carou, D., Gapinski, B., & Ramírez, I. (2023). Characterization of 5356 aluminum walls produced by wire arc additive manufacturing (WAAM). Materials, 16(7), 2570. https://doi.org/10.3390/ma16072570

Yang, Y., Gong, Y., Qu, S., Rong, Y., Sun, Y., & Cai, M. (2018). Densification, surface morphology, microstructure and mechanical properties of 316L fabricated by hybrid manufacturing. International Journal of Advanced Manufacturing Technology, 97(5–8), 2687–2696. https://doi.org/10.1007/s00170-018-2144-1

Zhang, H., Li, R., Liu, J., Wang, K., Weijian, Q., Shi, L., Lei, L., He, W., & Wu, S. (2024). State-of-art review on the process-structure-properties-performance linkage in wire arc additive manufacturing.

https://doi.org/10.24191/jmeche.v23i1.7015

Virtual and Physical Prototyping, 19(1), e2390495. https://doi.org/10.1080/17452759.2024.2390495

Zhang, S., Gong, M., Cen, L., Lu, Y., & Gao, M. (2023). Differences in properties between hybrid wire arc additive-milling subtractive manufactured aluminum and magnesium alloys. Applied Sciences, 13(4), 2720. https://doi.org/10.3390/app13042720

Zhang, T., Li, H., Gong, H., Ding, J., Wu, Y., Diao, C., Zhang, X., & Williams, S. (2022). Hybrid wire - arc additive manufacture and effect of rolling process on microstructure and tensile properties of Inconel 718. Journal of Materials Processing Technology, 299, 117361. https://doi.org/10.1016/j.jmatprotec.2021.117361

Zhou, Y., Lin, X., Kang, N., Huang, W., Wang, J., & Wang, Z. (2020). Influence of travel speed on microstructure and mechanical properties of wire + arc additively manufactured 2219 aluminum alloy. Journal of Materials Science and Technology, 37, 143–153. https://doi.org/10.1016/j.jmst.2019.06.016

https://doi.org/10.24191/jmeche.v23i1.7015